Temperature dependence of the order parameter of cuprate superconductors

Alexander Mihlin and Assa Auerbach
Physics Department, Technion, Haifa 32000, Israel

(Received 14 July 2009; revised manuscript received 15 September 2009; published 26 October 2009)

A model of charged hole-pair bosons with long-range Coulomb interactions and very weak interlayer coupling is used to calculate the order parameter Φ of underdoped cuprates. Model parameters are extracted from experimental superfluid densities and plasma frequencies. The temperature dependence $\Phi(T)$ is characterized by a "*trapezoidal*" shape. At low temperatures, it declines slowly due to harmonic phase fluctuations which are suppressed by anisotropic plasma gaps. Above the single layer Berezinski-Kosterlitz-Thouless temperature, $\Phi(T)$ falls rapidly toward the three-dimensional transition temperature. The theoretical curves are compared to *c*-axis superfluid density data by Kitano *et al.* [J. Low Temp. Phys. **117**, 1241 (1999)] and to the *transverse nodal velocity* measured by angular resolved photoemission spectra on BSCCO samples by Lee *et al.* [Nature (London) **450**, 81 (2007)] and by Kanigel *et al.* [Phys. Rev. Lett. **99**, 157001 (2007)].

DOI: 10.1103/PhysRevB.80.134521 PACS number(s): 74.72.−h, 74.20.−z, 74.78.Fk

I. INTRODUCTION

Unconventional superconductivity in cuprates is often measured by deviations from the phenomenology of Bardeen, Cooper, and Schrieffer (BCS).[1] A case in point is the order parameter

$$\Phi(T) = \sum_{\boldsymbol{\eta}} d(\boldsymbol{\eta}) \langle c^{\dagger}_{\mathbf{r}\uparrow} c^{\dagger}_{\mathbf{r}+\boldsymbol{\eta}\downarrow} \rangle, \tag{1}$$

where $d(\boldsymbol{\eta})$ is the intralayer pairing function with *d*-wave symmetry, and uniformity is assumed in suppressing the $\mathbf{r}$ dependence of Φ. In BCS theory, the order parameter is inextricably related to a *gap in the quasiparticle excitations*, whose maximal value is given by

$$\Delta_{\mathrm{BCS}}(T) = \bar{V}\Phi(T). \tag{2}$$

where $\bar{V}$ is an interaction parameter. Δ_{BCS} is the pair breaking energy which sets the scale of the transition temperature T_c. However, BCS theory is a mean-field approximation which neglects all phase fluctuations.

In underdoped cuprates, there is compelling evidence that T_c is driven by phase fluctuations.[2] Uemura's empirical scaling law $T_c \propto \rho_s^{ab}(T=0)$ (Ref. 3) and the observation of a superfluid density jump in ultrathin underdoped cuprate films[4–7] are consistent with the behavior of a bosonic superfluid, captured by an effective *xy* model.

In this paper we calculate the temperature-dependent order parameter of an effective Hamiltonian of charged lattice bosons (CLBs). The CLB model incorporates essential ingredients of underdoped cuprates including extremely weak interlayer coupling and long-range Coulomb interactions.

Our main result is that $\Phi(T)$ exhibits a *trapezoidal shape* in the weak interlayer coupling limit, as depicted in Fig. 1. At low temperatures $\Phi(T)$ decreases slowly due to effects of anisotropic plasma frequency gaps. The effects of long-range charge interactions, however, do not drive the transition. The transition is driven by proliferation of vortex loops above the two-dimensional Berezinskii-Kosterlitz-Thouless (BKT) (Ref. 8) temperature T_{BKT}, where the order parameter falls rapidly toward T_c.

Phase fluctuation theories have been previously applied to cuprates, with special attention to the intralayer superfluid density $\rho_s^{ab}(T)$.[9–11] In order to explain the linearly decreasing temperature dependence, additional gapless (nodal) fermionic excitations were argued to be essential.[12]

$\Phi(T)$, however, behaves differently than $\rho_s^{ab}(T)$. In the two-dimensional (2D) limit, for example, Φ must vanish at all $T>0$ by Mermin and Wagner theorem,[13] while ρ_s^{ab} jumps to a finite value below T_{BKT}. Also, nodal fermions have a small effect on $\Phi(T)$. This is demonstrated in Fig. 1, which shows *s* and *d* wave order parameters behaving very similarly within BCS theory.

We propose experimental probes for the order parameter without relying on BCS theory and Eq. (2). At weak interlayer coupling, we argue that $\Phi(T)$ should be proportional to the square root of the *c*-axis superfluid density.

Angular-resolved photoemission spectroscopy (ARPES) finds a "*pseudogap*" Δ_{pg} in the electronic spectrum, which persists well above T_c.[14–16] Apparently, $\Delta_{pg}(T)$ is *not* propor-

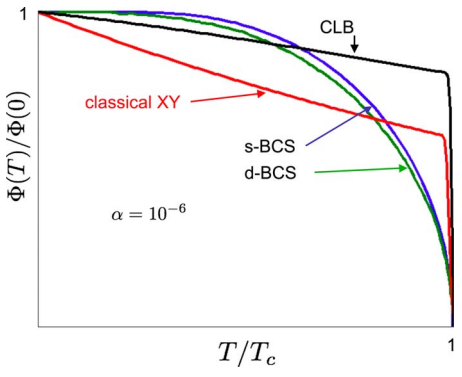

FIG. 1. (Color online) Temperature dependences of normalized superconducting order parameters. A *trapezoidal* shape is obtained for charged lattice bosons (black) model [Eq. (5)] for anisotropy ratio $\alpha=10^{-6}$ and $\kappa=150$. We see that coulomb interactions suppress thermal phase fluctuations relative to the classical *xy* model [Eq. (3)] (red) depicted for $\alpha=10^{-6}$. The rapid fall toward T_c is calculated within interlayer mean-field theory (see text). BCS theory for *d*- and *s*-wave order parameters is depicted for comparison, (green and blue, respectively).

tional to $\Phi(T)$ (the latter of course vanishes at T_c), which violates Eq. (2). Pseudogap phenomena are often interpreted as *short-range pairing correlations* well above T_c.

To address ARPES data, we employ a Boson-Fermion (BF) model which was derived from the Hubbard model[17] by contractor renormalization. The model describes the CLB system, Andreev-coupled to fermion quasiparticles which occupy small hole pockets (or "arcs").

Other BF models have been proposed to handle tightly bound pairs in polaronic,[18] cuprate,[19] and disordered superconductors.[20] Recent advances have been made using BF models for cold fermion atoms with attractive interactions.[21] Field theoretical versions were also studied.[22,23]

Within the specific model we propose, $\Phi(T)$ turns out to be directly proportional to the *transverse nodal velocity* $v_\perp(T)$.[24] In Fig. 5, we find reasonable agreement between the theoretical curves and $Bi_2Sr_2CaCu_2O_{8+\delta}$ (BSCCO) ARPES data for $v_\perp(T)$ of Refs. 25 and 26. Further tests of the trapezoidal shape closer to T_c would be desirable.

The paper is organized as follows: The CLB model is introduced in Sec. II. The order parameter is calculated within the harmonic phase fluctuations approximation to obtain the low-temperature regime. In Sec. III, the interlayer mean-field theory is applied to compute the suppression of the order parameter near T_c. In Sec. IV we relate the model parameters to experimental data for several commonly studied cuprates. Section V compares the theory to experiments using an effective Boson-Fermion model to interpret the ARPES data. We conclude with a brief summary and discussion.

In Appendix A, we provide details of the analytical fit to the harmonic phase fluctuations result. In Appendix B we estimate the temperature region near T_c where three-dimensional critical fluctuations are important (Ginzburg criterion).

II. CHARGED LATTICE BOSONS

The xy Hamiltonian is a lattice model of boson phase fluctuations,

$$\mathcal{H}_{xy} = -\frac{J}{2}\left[\sum_{\mathbf{r},\boldsymbol{\eta}} \cos(\varphi_{\mathbf{r}} - \varphi_{\mathbf{r}+\boldsymbol{\eta}}) + \alpha \sum_{\mathbf{r},\mathbf{c}} \cos(\varphi_{\mathbf{r}} - \varphi_{\mathbf{r}+\mathbf{c}})\right], \tag{3}$$

where $\mathbf{r}$ resides on a layered tetragonal lattice. $\boldsymbol{\eta}$ and $\mathbf{c}$ are in-plane and interlayer nearest-neighbor vectors of lengths a and c, respectively. The lattice constant a is in effect a coarse-grained parameter chosen to be larger than the coherence length ξ. J is the bare intralayer superfluid density, and $\alpha \ll 1$ is the anisotropy ratio.

The order parameter is defined by

$$\Phi(T) = \Phi_0 \langle \cos(\varphi_{\mathbf{r}}) \rangle, \tag{4}$$

where Φ_0 is the zero-temperature value. The quantum CLB model is given by

$$\mathcal{H}_{clb} = \mathcal{H}_{xy}[\varphi] + \frac{1}{2}\sum_{\mathbf{r},\mathbf{r}'} V(\mathbf{r}-\mathbf{r}') n_{\mathbf{r}} n_{\mathbf{r}'}, \tag{5}$$

where $n_{\mathbf{r}}$ is the occupation number of a charge $2e$ boson on site $\mathbf{r}$, obeying the commutation relation,

$$[n_{\mathbf{r}}, \varphi_{\mathbf{r}'}] = i\delta_{\mathbf{r},\mathbf{r}'}. \tag{6}$$

Long-range Coulomb interactions $V(\mathbf{r})$ are given by the Fourier components

$$V_{\mathbf{q}} = \sum_{\mathbf{r}} e^{-i\mathbf{q}\mathbf{r}} V(\mathbf{r}) = \frac{16\pi e^2}{v\epsilon_b q^2}, \tag{7}$$

where $v \equiv a^2 c$ is a unit-cell volume and $\epsilon_b(\mathbf{q}, \omega_{\mathbf{q}})$ is the effective dielectric function in the appropriate wave vector and frequency scale.

At low temperatures, we can expand the CLB action to quadratic order and obtain the harmonic phase fluctuations (HPF) action,

$$\mathcal{S}_{hpf}[\varphi] = \frac{1}{2}\hbar^2 T \sum_{\mathbf{q}n} \frac{\omega_n^2 + \omega_p^2(\mathbf{q})}{V_{\mathbf{q}}} \varphi_{\mathbf{q}\omega_n} \varphi_{-\mathbf{q}-\omega_n}, \tag{8}$$

where $\omega_n = 2\pi n T/\hbar$ are bosonic Matsubara frequencies. The plasmon dispersion,\ as derived by Kwon *et al.*[10] is

$$\omega_p^2(\mathbf{q}) \equiv \frac{\omega_{ab}^2 q_{ab}^2 + \omega_c^2 q_c^2}{q^2},$$

$$\omega_{ab}^2 = \frac{16\pi e^2 J}{\epsilon_b \hbar^2 c},$$

$$\omega_c^2 = \frac{16\pi e^2 c \alpha J}{\epsilon_b \hbar^2 a^2}, \tag{9}$$

where q_{ab} and q_c are the planar and c-axis wave vectors, respectively.

The HPF order parameter is given by

$$\Phi_{\mathrm{HPF}}(T) = \Phi_0 e^{-1/2\langle \varphi_{\mathbf{r}}^2 \rangle}, \tag{10}$$

where the local phase fluctuations are given by

$$\langle \varphi_{\mathbf{r}}^2 \rangle = \frac{1}{Z}\int \mathcal{D}\varphi \varphi_{\mathbf{r}}^2 e^{-\mathcal{S}_{hpf}(\varphi)} = v\int \frac{d^3q}{(2\pi)^3} \frac{V_{\mathbf{q}}}{\hbar\omega_p(\mathbf{q})} \left\{ \frac{\sinh[\hbar\omega_p(\mathbf{q})/T]}{\cosh[\hbar\omega_p(\mathbf{q})/T] - 1} \right\}. \tag{11}$$

At extremely low temperatures, $T \ll \hbar\omega_c$, all thermal phase fluctuations are frozen out. However, as we shall show in Sec. V, the experimentally interesting regime of large anisotropy has a wide separation of plasma energy scales, such that

$$\hbar\omega_c \ll T_{\mathrm{BKT}} \sim T_c \ll \hbar\omega_{ab}. \tag{12}$$

For our regime, we fit Eq. (11) by the analytical approximation (see Appendix A),

$$\langle \varphi^2 \rangle_{T,\alpha} = \left(\frac{T}{J}\right)(a_1 - a_2|\ln(\alpha)|)e^{-a_3\hbar\sqrt{\omega_{ab}\omega_c}/T}. \quad (13)$$

For the simplified case of $a=c$, the coefficients are given by

$$a_1 \approx 0.045, \quad a_2 = -0.013,$$

$$a_3 \approx 0.35. \quad (14)$$

Thus, expression (10) reduces to the classical result of Hikami and Tsuneto (HT) (Ref. 27) [shown later in Eq. (24)] in the limit $T \gg a_3\hbar\sqrt{\omega_{ab}\omega_c}$. In the experimentally relevant regime, Φ_{HPF} decreases significantly slower than the classical model, as demonstrated in Fig. 1.

III. INTERLAYER MEAN FIELD THEORY

The HPF action [Eq. (8)] cannot describe the order parameter near T_c since it does not include vortex excitations. In the narrow regime of $T_{\mathrm{BKT}} \leq T \leq T_c$ proliferation of widely separated two-dimensional vortex pairs dramatically reduces the order parameter.

For anisotropies of order $\alpha \sim 10^{-4}-10^{-6}$, a straightforward numerical calculation of Eq. (3) is encumbered by finite-size limitations. Instead, we employ the interlayer mean-field theory (IMFT) (Ref. 28) described by a single layer Hamiltonian in an effective field h:

$$\mathcal{H}_{imft}(h) = \mathcal{H}_{2d}(h) + \frac{h^2}{2\alpha J},$$

$$\mathcal{H}_{2d}(h) = -J\sum_{\mathbf{r}\boldsymbol{\eta}}^{\mathrm{2D}} \cos(\varphi_{\mathbf{r}} - \varphi_{\mathbf{r}+\boldsymbol{\eta}}) - 2h\sum_{\mathbf{r}}^{\mathrm{2D}} \cos(\varphi_{\mathbf{r}}). \quad (15)$$

Variational determination of h yields the IMFT equation

$$h = 2\alpha J\langle \cos\varphi_{\mathbf{r}} \rangle = 2\alpha J\Phi_{2d}(T,h), \quad (16)$$

where the magnetization of a single two-dimensional layer, $\Phi_{2d}(T,h)$, is, in principle, the *exact* field dependent order parameter of the single layer CLB model. Solving Eq. (16) for $h(T)$, yields the three-dimensional temperature-dependent order parameter

$$\Phi_{imft}(T) = \Phi_{2d}[T,h(T)]. \quad (17)$$

The transition temperature T_c is given by

$$T_c = \min_T\{T;\Phi_{imft}(T)=0\}. \quad (18)$$

Solution of Eq. (16) for small anisotropies requires precise determination of $\Phi_{2d}(T,h)$ for very weak fields h near T_c. This is obtained by using the asymptotic critical properties of the order parameter near T_{BKT}, which is not far from T_c in the small α limit.

A. BKT critical properties

The two-dimensional classical xy model undergoes a BKT transition[8] at $T_{\mathrm{BKT}} \approx 0.89\ J$.[56,57] Vortex pair proliferation changes the phase correlation temperature dependence from power law to exponential decay,

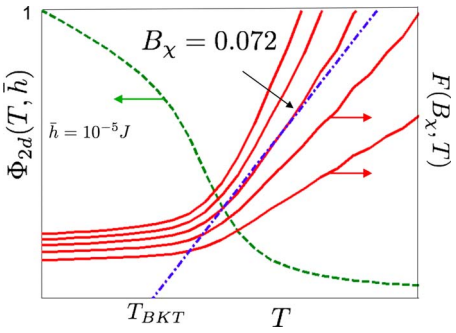

FIG. 2. (Color online) Determination of B_χ from Monte Carlo data. The different fitting functions $F(B_\chi,T)$ (solid lines, red) are defined in Eq. (22). The curve with parameter value $B_\chi=0.072$ is chosen as the best fit to $(T-T_{\mathrm{BKT}})/T_{\mathrm{BKT}}$. The dashed (green) line is the two-dimensional order parameter in the presence of an ordering field $\bar{h}$.

$$\langle \cos(\varphi_{\mathbf{r}} - \varphi_0)\rangle \sim \begin{cases} r^{-\eta(T)} & T < T_{\mathrm{BKT}} \\ e^{-r/\xi(T)} & T > T_{\mathrm{BKT}}, \end{cases} \quad (19)$$

where at low temperatures,

$$\eta \simeq \frac{T}{2\pi J}, \quad T \ll T_{\mathrm{BKT}}. \quad (20)$$

Above T_{BKT} the correlation length diverges as

$$\xi_{2d} \propto \exp(\beta/\sqrt{t}),$$

$$\chi_{2d}(t) = \frac{B_\chi}{J}\exp(\nu\beta/\sqrt{t}),$$

$$t \equiv (T - T_{\mathrm{BKT}})/T_{\mathrm{BKT}},$$

$$\beta = 3/2, \quad \nu = 7/4, \quad (21)$$

where the exponents β and ν were derived by Kosterlitz.[31]

In order to match the transition region to the low-temperature HPF order parameter, we need to determine the nonuniversal amplitude B_χ of $\chi_{2d}(T)$. B_χ was determined numerically. We evaluated $\Phi_{2d}(T,\bar{h}=10^{-5}J)$ by a Monte Carlo simulation with Hamiltonian (15). System size with 50×50 sites. Good convergence was achieved with 10^9 spin tilts per (T,h) point, sampling every 10^5 tilts and averaging over the last 5000 configurations. We define a fitting function

$$F(B_\chi,T) = \left\{\frac{\nu\beta}{\ln[J\Phi_{2d}(T,\bar{h})/(\bar{h}B_\chi)]}\right\}^2. \quad (22)$$

The fitting procedure which is depicted in Fig. 2 yields

$$B_\chi \simeq 0.072. \quad (23)$$

For finite interlayer coupling, the classical xy model orders at $T_c(\alpha) > T_{\mathrm{BKT}}$. Hikami and Tsuneto[27] evaluated the order parameter for small $\alpha \ll 1$ and obtained

$$\Phi_{cl}(T) = \Phi_0\alpha^{\eta/(4-2\eta)} \simeq \Phi_0 e^{-T/8\pi J|\ln\alpha|}. \quad (24)$$

In Fig. 1, $\Phi_{cl}(T)$ of Eq. (24) is plotted in comparison to the CLB model. The classical model decreases much faster since

it does not contain the plasma gaps in the thermal phase fluctuations.

The IMFT equation for T_c is

$$2\alpha J\chi_{2d}(T_c) = 1. \tag{25}$$

Using Eq. (21) for $\chi_{2d}(T)$ and the value [Eq. (23)] for B_χ, the shift of T_c is

$$T_c - T_{BKT} \sim \left[\frac{\beta\nu}{\ln(2B_\chi\alpha)}\right]^2 T_{\mathrm{BKT}}. \tag{26}$$

The IMFT is consistent with the renormalization group analysis of Hikami and Tsuneto.[27] We note, however, that a large vortex core energy can increase the shift of T_c above the value given by Eq. (26).[29,30]

The critical-field exponent was derived by Kosterlitz[31]

$$\Phi_{2d}(T_{\mathrm{BKT}}) \propto h^{1/\delta}, \quad \delta = 15. \tag{27}$$

Combining this result with the IMFT Eq. (16) yields

$$\Phi(T_{\mathrm{BKT}}) \propto \alpha^{1/(\delta-1)} = \alpha^{1/14}. \tag{28}$$

Thus, by Eqs. (26) and (28), the order parameter drops rapidly between T_{BKT} and T_c, with an average slope of $d\Phi(T)/dT \sim -|\ln(\alpha)|^2$.

B. Matching at the crossover

In the crossover region, Φ_{2d} is given by the *harmonic mean* of the temperature- and field-dependent singularities at T_{BKT},

$$\Phi_{2d}(T,h) = \Phi_{\mathrm{HPF}}(T)\left[\frac{1}{h\chi_{2d}(T)} + \left(\frac{h_0}{h}\right)^{1/\delta}\right]^{-1}. \tag{29}$$

Equation (29) correctly captures the singularities of the variables (t,h) at the BKT transition. h_0 is chosen to match the order parameter smoothly at T_{BKT},

$$h_0 = 2\alpha J\Phi_{\mathrm{HPF}}(T_{\mathrm{BKT}}). \tag{30}$$

IMFT as a mean-field theory cannot properly capture *three-dimensional* critical exponents of the *xy* model. Nevertheless, as shown in Appendix B, the critical regime by Ginzburg's criterion is limited to

$$T_c - T < T_{\mathrm{BKT}}/|\ln\,\alpha|^4, \tag{31}$$

which is difficult to resolve experimentally, in the systems of interest.

C. Fermionic excitations

The CLB model ignores effects of fermionic particle-hole excitations, which are clearly observed in ARPES and tunneling. In underdoped cuprates, most of their spectral weight is associated with wave vectors around the antinodes $[(\pi,0),(0,\pi)]$ with energies at the pseudogap scale $\Delta_{pg} \gg T_c$. Contribution of these excitations to depletion of the order-parameter temperature is of order $T/\Delta_{pg} \ll 1$.

Nevertheless, one might worry that *low energy* (nodal) excitations might play an important role. This has been shown to be the case for the temperature dependence of the superfluid density $\rho_s^{ab}(T)$.[9,11,32]

However, nodal excitations are weakly coupled to the order parameter. Consider, for example, the BCS gap equation,

$$\frac{1}{\lambda} = \sum_{\mathbf{k}} \frac{|d(\mathbf{k})|^2}{E_{\mathbf{k}}[\Delta(T)]}\tanh[E_{\mathbf{k}}(\Delta(T))/T], \tag{32}$$

where

$$E_{\mathbf{k}} = \sqrt{(\epsilon_{\mathbf{k}} - \mu)^2 + |d(\mathbf{k})\Delta(T)|^2} \tag{33}$$

and λ is the BCS coupling constant. The pair wave-function factor $|d(\mathbf{k})|^2$ vanishes on the nodal lines $\mathbf{k}=(\pm k,k)$. This suppresses contributions from the nodal regions to the thermal depletion of the gap. As a result, *s*-wave and *d*-wave order parameters have very similar temperature dependence as shown by Won and Maki[33] and depicted in Fig. 1. Although here we do not appeal to BCS theory, this observation depends only on the weak coupling between nodal fermions and the order parameter imposed by the pair wave-function symmetry.

IV. EXPERIMENTAL PARAMETERS

The cuprates exhibit very large anisotropy between in-plane and interlayer Josephson couplings J_c and J_{ab}, which can be experimentally determined by the in-plane and interlayer zero-temperature London penetration depths λ_{ab}^0 and λ_c^0,

$$\lambda_{ab}^0 = \left(\frac{16\pi e^2}{\hbar^2 c^2 d} J_{ab}\right)^{-1/2},$$

$$\lambda_c^0 = \left(\frac{16\pi e^2 d}{\hbar^2 c^2 a^2} J_c\right)^{-1/2}, \tag{34}$$

where d and a are effective lattice constants, e is the electron charge, and c is the speed of light. The anisotropy ratio for cuprates is in the range,

$$\alpha \equiv \frac{J_c}{J_{ab}} = \left(\frac{\lambda_{ab}^0 a}{\lambda_c^0 d}\right)^2 \sim 10^{-6} - 10^{-3}. \tag{35}$$

Our phenomenological assignment of J_{ab} and J_c neglects quantum corrections which become sizable near the critical doping toward the insulating phase. An alternative measure of J_{ab} and J_c is given by relations (9) and the experimental measurements of ω_{ab} and ω_c by optical and microwave conductivities (cf. Refs. 34–44). Thus, the anisotropy parameter, α, of Eq. (35) can be determined.

Table I contains typical experimental values of relevant quantities at zero temperature [except for Ω and α which were determined via Eqs. (A6) and (35), respectively]. In $YBa_2Cu_3O_{7-\delta}$, BSCCO, and $Tl_2Ba_2CaCu_2O_{8+\delta}$, the interplane distance c is taken as the mean value.

V. EXPERIMENTAL PROBES OF $\Phi(T)$

In cuprates, the BCS relation [Eq. (2)] does not hold, since the maximal gap Δ_{pg} is weakly temperature

TABLE I. Typical planar lattice constants, a, mean interplane distances, c, critical temperatures, T_c, planar and interplane plasma frequencies, ω_{ab}, ω_c, energy scales $\Omega(\alpha,a,c)$ of Eq. (13), magnetic field penetration depths, λ_{ab}, λ_c, and anisotropy factors, α, at zero temperature. All quantities except for $\Omega(\alpha,a,c)$ and α were obtained experimentally, while Ω and α were obtained via Eqs. (A6) and (35), respectively. Some quantities depend on doping (e.g., λ_{ab} and λ_c are diminished with doping) and values for each compound correspond to similar dopings.

Compound	a (A)	c (A)	T_c (K)	$\hbar\omega_{ab}$ (eV)	$\hbar\omega_c$ (meV)	Ω (meV)	λ_{ab} (μm)	λ_c (μm)	α (10^{-4})	Ref.
$YBa_2Cu_3O_{7-\delta}$	3.8	5.8	89	1.5–2.5	5.6–13.6	36.1–72.3	0.14–0.28	1.26–7.17	50–5	34, 40, 41, and 47
$Bi_2Sr_2CaCu_2O_{8+\delta}$	5.4	7.7	92	0.94–1.84	0.23–1.4	5.6–19.5	0.2	110	0.016	35, 36, 42, and 48
$La_{2-\delta}Sr_\delta CuO_4$	3.8	6.6	40	0.3–3	3.7–11.2	13–75.4	0.19–0.28	2–8.5	30–3	16, 37, 38, 40, 43, and 49
$Tl_2Ba_2CaCu_2O_{8+\delta}$	3.9	7.4	108	1.5	1.2–2.6	17.4–26.8	0.17–0.33	2.5–8.4	13–4	39, 44, and 50

dependent,[15,46] while $\Phi(T)$ vanishes at T_c. Here we propose experimental probes to measure $\Phi(T)/\Phi(0)$.

A. *c*-axis superfluid density

Since the zero-temperature interlayer pair tunneling is weak, the layered system can be treated as a one-dimensional array of Josephson junctions. Within a variational approximation, the order parameter can be extracted from the temperature dependence of the c-axis superfluid density,

$$\rho_s^c(T) = \rho_s^c(0)|\Phi(T)|^2. \tag{36}$$

Indeed, as seen in Fig. 3, agreement between theoretical curves $\Phi(T)$ and values extracted from electrodynamical data of BSCCO (Ref. 45) are quite good except near the transition.

B. ARPES

In d-wave BCS theory the quasiparticle spectrum is given by Eq. (33). Above T_c, $\Delta_{BCS}=0$, and the full Fermi surface should be detected as zero energy crossings of the ARPES quasiparticle peaks. However, in underdoped cuprates as temperature is raised above T_c, only finite Fermi arcs appear around the nodal directions. The gap in the antinodal directions Δ_{pg} survives to much higher temperatures.[15,46] In contrast to Δ_{pg}, the transverse nodal velocity $v_\perp$ vanishes abruptly at T_c.[25,26] Below T_c, $v_\perp$ introduces a singularity $|k_\perp|$ in the electronic propagator, which translates to an infinite correlation length in real space.

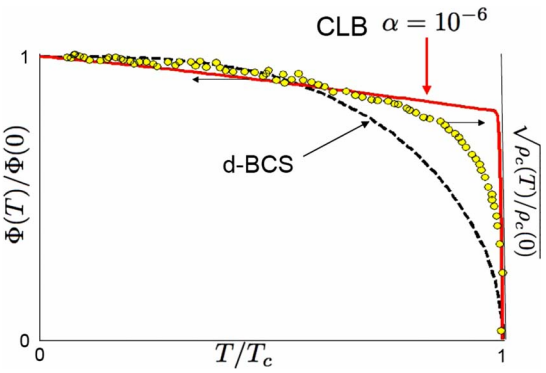

FIG. 3. (Color online) Comparison of CLB order parameter to square root of c-axis superfluid density from Ref. 45. Model parameters are $\alpha=10^{-6}$, $c/a=0.5$, and $\kappa\equiv\omega_{ab}/J=150$. Data was taken on BSCCO with $T_c=87$ K. Dashed line is d-wave BCS energy gap, given for comparison.

A microscopic connection between $v_\perp(T)$ and $\Phi(T)$ can be provided by an effective Boson-Fermion Hamiltonian with small hole pockets described below.

C. Boson-Fermion theory

The BF model, which arises by a contractor renormalization of the square lattice Hubbard model,[17] describes spin-half fermion holes $f_{\mathbf{k},s}$ of charge e coupled to the CLB as

$$\mathcal{H}_{bf} = \mathcal{H}_{clb} + \sum_{\mathbf{k},s} (\epsilon_{\mathbf{k}}^h - \mu) f_{\mathbf{k}s}^\dagger f_{\mathbf{k}s} + g \sum_{\mathbf{r},\mathbf{r}'} e^{i\varphi_{\mathbf{r}}} d(\mathbf{r}-\mathbf{r}') f_{\mathbf{r},\uparrow} f_{\mathbf{r}',\downarrow} + \text{H.c.} \tag{37}$$

The last Andreev coupling term, describes disintegration of hole pairs into single spin-half hole fermions. In our version of the BF model, the fermion and boson densities measured with respect to half filling obey

$$n_h + 2n_b = x, \tag{38}$$

where x is the total concentration of doped holes. The hole dispersion $\epsilon_{\mathbf{k}}$ has minima near $(\pm\pi/2, \pm\pi/2)$ and therefore occupy four *small* pockets of area fraction $n_h/2$. The low hole density count distinguishes Eq. (37) from BF models with high fermion densities (large Fermi surfaces) as defined in Refs. 18, 21, and 22.

Above T_c, the small wave vector sides of the pockets appear as the celebrated Fermi arcs.[24,51] The pseudogap is given by the quasiparticle excitation energy at the antinodal wave vectors

$$\Delta_{pg} = \epsilon_{(\pi,0)} - \mu. \tag{39}$$

In the superconducting phase $\Phi(T)=\langle\cos(\varphi)\rangle$. The hole fermions acquire the Dirac cone dispersion near the nodes:

$$E_{\mathbf{k}} = \pm\sqrt{[v_F(k_\parallel - k_F)]^2 + [2g\Phi(T)k_\perp]^2} \tag{40}$$

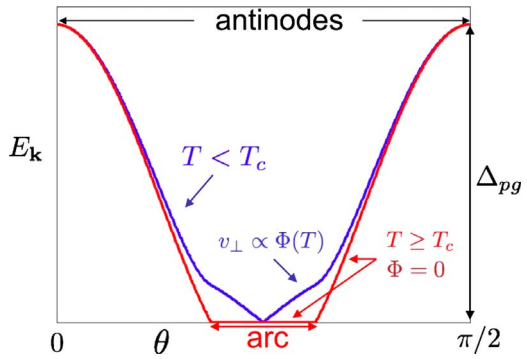

FIG. 4. (Color online) Boson-Fermion model for the transverse quasiparticle excitations below and above T_c. θ is the azimuthal coordinate transverse to the nodal direction. Above T_c (red), vanishing of $E_{\mathbf{k}}$ on a finite arc reflects the inner edge of the hole pocket. The pseudogap Δ_{pg} is the hole fermions energy at the antinodal wave vectors $(\pi,0),(0,\pi)$, which has no direct bearing on the superconducting properties. Below T_c (blue), the Andreev coupling of hole fermions to hole-pair bosons yields a d-wave gap with a node at $\theta=0$. The transverse nodal velocity $v_\perp(T)$ is a direct measurement of $\Phi(T)$. The break in the curve at the arc edge is consistent with two gaps phenomenology (Ref. 52).

that is depicted in Fig. 4. Thus, the transverse velocity directly measures the order parameter,

$$v_\perp(T) = 2g\Phi(T). \tag{41}$$

In the underdoped regime, the transverse velocity is smaller than the pseudogap scale $\Delta_{pg}d'(\mathbf{k})$. This is seen as a break in $E_{\mathbf{k}}$ at the Fermi arcs angles, as shown in Fig. 4. Such behavior has been observed in ARPES (Ref. 52) and found consistent with a two gap phenomenology.

In Fig. 5 we compare the CLB order parameter to the transverse nodal velocities measured on three samples of

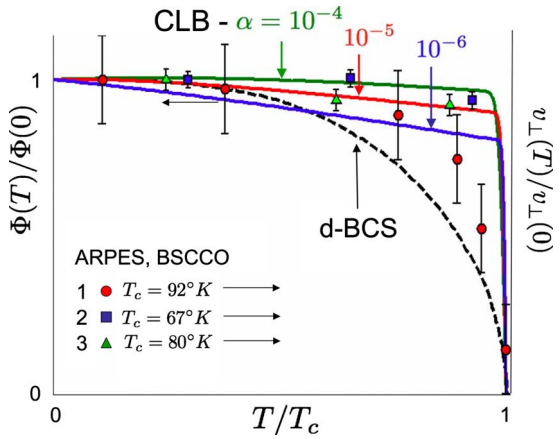

FIG. 5. (Color online) Comparison of CLB to transverse nodal velocity measured on different samples by ARPES. BSSCO samples with T_c noted in the figure. Experimental data, including error bars, are (1) from Ref. 25 and [(2) and (3)] from Ref. 26. The zero-temperature normalization is chosen by the lowest temperature data points. Theoretical curves for several values of α are drawn. using $c/a=0.5$ and $\kappa \equiv \omega_{ab}/J=150$. Dashed line is d-wave BCS energy gap, given for comparison.

BSSCO by two groups.[25,26] The agreement is reasonable although the sharp break in the curves is not clearly confirmed. A comparison to the d-wave BCS expression shows a systematic trend of all the data being higher than BCS theory would predict.

VI. DISCUSSION

This paper calculated the order parameter of cuprates using a bosonic model of hole pairs. The model includes crucial features of layered cuprates: long-range Coulomb interactions and very small anisotropy ratio. It ignores effects of fermionic particle hole excitations which are argued to be small for $\Phi(T)$. The calculation predicts a trapezoidal temperature dependence in the small α limit, which is distinct from both BCS theory and the classical xy model. The theoretical curves are compared to data where the order parameter is extracted by additional theoretical assumptions: the c-axis superfluid density (using a variational argument) and the transverse nodal velocity (using a BF model of small hole pockets). We have selectively chosen data of BSCCO where $\alpha=10^{-6}$, and the trapezoidal temperature dependence is most pronounced. In other cuprates, with larger values of α, and larger vortex core energies[29] the shift T_c-T_{BKT} is larger, and the curve should be more rounded (less trapezoidal) and similar to the BCS curve.

Additional probes to $\Phi(T)$ could be devised. The critical current of a c-axis Josephson junctions with a higher T_c material might be investigated. The transverse nodal velocity, which we have related to Φ by the BF theory, determines the low-energy tunneling spectra and Raman scattering.[53] In addition, it has been theoretically related to the linear slope of the superfluid density $d\rho_s^{ab}/dT$ (Ref. 32) and to thermal conductivity.

Further comparisons to experiments are warranted. Their success or failure may shed light on the applicability of the quantum lattice bosons description of cuprates both below and above T_c. This would help us resolve some of the other mysteries of the pseudogap phase.

ACKNOWLEDGMENTS

We thank Ehud Altman, Thierry Giamarchi, Amit Kanigel, Amit Keren, and Christos Panagopoulos for useful advice and information. A.A. acknowledges support from the Israel Science Foundation and is grateful for the hospitality of Aspen Center for Physics where some of the ideas were conceived.

APPENDIX A: FITTING PHASE FLUCTUATIONS

We define $q^2 \equiv q_c^2 + q_{ab}^2$, $\eta^2 \equiv (\omega_c/\omega_{ab})^2 = \alpha\gamma^2$, and $\gamma \equiv c/a$. For ease of numerical integration Eq. (11) may be simplified as follows:

$$\langle \varphi_{\mathbf{li}}^2 \rangle = \frac{1}{Z}\int \mathcal{D}\varphi \varphi_{\mathbf{li}}^2 e^{-\mathcal{S}^{(2)}(\varphi)}$$

$$= v\int \frac{d^3q}{(2\pi)^3}\frac{V_{\mathbf{q}}}{\hbar\omega_p(\mathbf{q})}\left\{\frac{\sinh[\beta\hbar\omega_p(\mathbf{q})]}{\cosh[\beta\hbar\omega_p(\mathbf{q})]-1}\right\}, \quad \text{(A1)}$$

$$\approx \frac{\gamma\hbar\omega_{ab}}{2\pi^2 J}\int_0^{\gamma\pi} dz \int_0^{\pi} dr \frac{r}{(z^2+r^2)\varepsilon\left(\eta,\frac{z}{r}\right)} \times \frac{\sinh\left[\varepsilon\left(\eta,\frac{z}{r}\right)/T\right]}{\cosh\left[\varepsilon\left(\eta,\frac{z}{r}\right)/T\right]-1}, \quad \text{(A2)}$$

where the last expression was obtained in cylindrical coordinates. The dispersion is thus parametrized by

$$\varepsilon\left(\eta,\frac{z}{r}\right) \equiv \hbar\omega_{ab}\sqrt{\frac{1+\eta^2(z/r)^2}{1+(z/r)^2}}. \quad \text{(A3)}$$

At extremely low temperatures, $T \ll \hbar\omega_c$, all thermal phase fluctuations are frozen out. However, due to the large anisotropy, and poor screening, there is a wide separation of energy scales between the interplane plasma gap, $\hbar\omega_c$, and the planar gap, $\hbar\omega_{ab}$, and it turns out that

$$\hbar\omega_c \ll T_c \sim J \ll \hbar\omega_{ab}. \quad \text{(A4)}$$

At low temperatures, the integral in Eq. (11) may be parametrized as

$$\langle \varphi^2 \rangle \approx \frac{AT}{J}e^{\Omega/T}, \quad \text{(A5)}$$

where the energy scale, $\Omega(\alpha,\gamma)$, and the coefficient $A(\alpha,\gamma)$ may be parametrized by

$$\Omega(\alpha,\gamma) \approx \hbar\left(\frac{0.09}{\sqrt{\gamma}}+0.26\sqrt{\gamma}\right)\sqrt{\omega_{ab}\omega_c} \quad \text{(A6)}$$

and

$$A(\alpha,\gamma) \approx A_1(\gamma) - A_2(\gamma)\ln(\alpha),$$

$$A_1(\gamma) \approx 0.029\gamma + 0.016\gamma^2,$$

$$A_2(\gamma) \approx 0.24\gamma - 0.11\gamma^2. \quad \text{(A7)}$$

The low-temperature magnetization, $\Phi_{hpf}(T)$, is given by

$$\Phi_{hpf}(T) \propto e^{-1/2\langle\varphi^2\rangle} = C(T)\alpha^{A_2 T/2J\exp(\Omega/T)}, \quad \text{(A8)}$$

where the coefficient $C(T)$ is given by

$$C(T) = e^{-A_1 T/2J\exp(\Omega/T)}. \quad \text{(A9)}$$

Notably, γ is of order unity and the energy scale, $\Omega(\alpha,\gamma)$, in Eq. (A5) is proportional to the geometric average of the interplane and planar plasma energies.

APPENDIX B: GINZBURG'S CRITERION FOR INTERLAYER MEAN-FIELD THEORY

One would like to know, in which regime can we trust the IMFT near the transition temperature. Here we estimate the critical region using the standard Ginzburg criterion. At small α, we see that the magnetization only varies rapidly below T_c, in the narrow region of width ΔT_c given by Eq. (26). Within that region, $\Phi_{imft}(T)$ drops from $\Phi_{\mathrm{HPF}}(T_{KT})$ as given by the harmonic phase fluctuations [Eq. (A8)] to zero at T_c with a mean-field behavior,

$$\Phi_{imft} \sim \Phi_{hpf}(T_{KT})\left(\frac{|T-T_c|}{\Delta T_c}\right)^{\beta}, \quad \beta = \frac{1}{2}. \quad \text{(B1)}$$

Ginzburg's criterion[54,55] estimates the temperature region below T_c, where critical 3D fluctuations become important and IMFT breaks down. This is where order-parameter fluctuations averaged over a correlation volume of size $V_\xi = \xi_{ab}^2\xi_c$ exceed their average, i.e.,

$$\langle(\Delta\Phi)^2\rangle_{V_\xi} = \frac{S(\mathbf{q}=0,T)}{V_\xi} = \frac{c}{\xi_c(T)} \geq \Phi_{imft}^2(T). \quad \text{(B2)}$$

Using the mean-field estimation of $\xi_c \sim c(|T-T_c|/T_c)^{-1/2}$ and Eq. (B1), the critical regime is given by

$$|T-T_c| \leq \Delta T_c^2/T_c \ll \Delta T_c, \quad \text{(B3)}$$

which is much smaller than the already narrow region of ΔT_c, where 2D vortex pair fluctuations suppress the order parameter. In summary, for layered systems with large anisotropy, IMFT theory holds up to temperatures very close to T_c.

[1] J. Bardeen, L. N. Cooper, and J. R. Schrieffer, Phys. Rev. **108**, 1175 (1957).

[2] V. J. Emery and S. A. Kivelson, Nature (London) **374**, 434 (1995).

[3] Y. J. Uemura, G. M. Luke, B. J. Sternlieb, J. H. Brewer, J. F. Carolan, W. N. Hardy, R. Kadono, J. R. Kempton, R. F. Kiefl, S. R. Kreitzman, P. Mulhern, T. M. Riseman, D. Ll. Williams, B. X. Yang, S. Uchida, H. Takagi, J. Gopalakrishnan, A. W. Sleight, M. A. Subramanian, C. L. Chien, M. Z. Cieplak, G. Xiao, V. Y. Lee, B. W. Statt, C. E. Stronach, W. J. Kossler, and X. H. Yu, Phys. Rev. Lett. **62**, 2317 (1989).

[4] A. K. Pradhan, S. J. Hazell, J. W. Hodby, C. Chen, Y. Hu, and B. M. Wanklyn, Phys. Rev. B **47**, 11374 (1993).

[5] M. B. Salamon, J. Shi, N. Overend, and M. A. Howson, Phys. Rev. B **47**, 5520 (1993); S. Kamal, D. A. Bonn, N. Goldenfeld, P. J. Hirschfeld, R. Liang, and W. N. Hardy, Phys. Rev. Lett. **73**, 1845 (1994); V. Pasler, P. Schweiss, C. Meingast, B. Obst, H. Wühl, A. I. Rykov, and S. Tajima, *ibid.* **81**, 1094 (1998); K. D. Osborn, D. J. Van Harlingen, V. Aji, N. Goldenfeld, S. Oh, and J. N. Eckstein, Phys. Rev. B **68**, 144516 (2003).

[6] T. Schneider, EPL **78**, 47003 (2007).

[7] I. Hetel, T. R. Lemberger, and M. Randeria, Nat. Phys. **3**, 700 (2007); Y. L. Zuev, J. A. Skinta, M. S. Kim, T. R. Lemberger, E. Wertz, K. Wu, and Q. Li, Physica C **468**, 276 (2008).

[8] V. L. Berezinskii, Zh. Eksp. Teor. Fiz. **61**, 1144 (1971); [Sov. Phys. JETP **34**, 610 (1972)]; J. M. Kosterlitz and D. J. Thouless, J. Phys. C **6**, 1181 (1973).
[9] A. Paramekanti, M. Randeria, T. V. Ramakrishnan, and S. S. Mandal, Phys. Rev. B **62**, 6786 (2000).
[10] H. J. Kwon, A. T. Dorsey, and P. J. Hirschfeld, Phys. Rev. Lett. **86**, 3875 (2001).
[11] M. Franz and A. P. Iyengar, Phys. Rev. Lett. **96**, 047007 (2006).
[12] I. F. Herbut and M. J. Case, Phys. Rev. B **70**, 094516 (2004).
[13] N. D. Mermin and H. Wagner, Phys. Rev. Lett. **17**, 1133 (1966).
[14] P. Curty and H. Beck, Phys. Rev. Lett. **91**, 257002 (2003).
[15] S. Hüfner, M. A. Hossain, A. Damascelli, and G. A. Sawatzky, Rep. Prog. Phys. **71**, 062501 (2008).
[16] C. Panagopoulos, J. R. Cooper, T. Xiang, Y. S. Wang, and C. W. Chu, Phys. Rev. B **61**, R3808 (2000).
[17] E. Altman and A. Auerbach, Phys. Rev. B **65**, 104508 (2002).
[18] J. Ranninger and S. Robaszkiewicz, Physica B **135**, 468 (1985).
[19] T. Kostyrko and J. Ranninger, Phys. Rev. B **54**, 13105 (1996).
[20] M. Cuoco and J. Ranninger, Phys. Rev. B **70**, 104509 (2004).
[21] A. V. Andreev, V. Gurarie, and L. Radzihovsky, Phys. Rev. Lett. **93**, 130402 (2004); V. Gurarie and L. Radzihovsky, Ann. Phys. **322**, 2 (2007).
[22] M. Franz and Z. Tesanovic, Phys. Rev. Lett. **87**, 257003 (2001); M. Franz, Z. Tesanovic, and O. Vafek, Phys. Rev. B **66**, 054535 (2002); Z. Tesanovic, Nat. Phys. **4**, 408 (2008).
[23] V. Galitski and S. Sachdev, Phys. Rev. B **79**, 134512 (2009).
[24] This is consistent with appearance of Fermi arcs above T_c, see: J. Ranninger and T. Domanski, arXiv:0904.2681 (unpublished).
[25] W. S. Lee, I. M. Vishik, K. Tanaka, D. H. Lu, T. Sasagawa, N. Nagaosa, T. P. Devereaux, Z. Hussain, and Z. X. Shen, Nature (London) **450**, 81 (2007).
[26] A. Kanigel, U. Chatterjee, M. Randeria, M. R. Norman, S. Souma, M. Shi, Z. Z. Li, H. Raffy, and J. C. Campuzano, Phys. Rev. Lett. **99**, 157001 (2007).
[27] S. Hikami and T. Tsuneto, Prog. Theor. Phys. **63**, 387 (1980).
[28] D. J. Scalapino, Y. Imry and P. Pincus, Phys. Rev. B **11**, 2042 (1975); See also R. Ofer, G. Bazalitsky, A. Kanigel, A. Keren, A. Auerbach, J. S. Lord, and A. Amato, *ibid.* **74**, 220508(R) (2006) for a more recent application.
[29] We note that in the detailed analysis of Benfatto *et al.*,[30] the effect of a large vortex core energy was emphasized. They have found that it can produce a large numerical factor in front of Eq. (26). Here we choose, for simplicity, to depict the results for the standard *xy* model keeping in mind that vortex core energy effects might be important for future comparisons with experiments.
[30] L. Benfatto, C. Castellani, and T. Giamarchi, Phys. Rev. Lett. **98**, 117008 (2007).
[31] J. M. Kosterlitz, J. Phys. C **7**, 1046 (1974).
[32] P. A. Lee and X.-G. Wen, Phys. Rev. Lett. **78**, 4111 (1997).
[33] H. Won and K. Maki, Phys. Rev. B **49**, 1397 (1994).
[34] G. A. Farnan, G. F. Cairns, P. Dawson, S. M. O'Prey, M. P. McCurry, and D. G. Walmsley, Physica C **403**, 67 (2004).
[35] T. Motohashi, K. M. Kojima, J. Shimoyama, S. Tajima, K. Kitazawa, S. Uchida, and K. Kishio, Phys. Rev. B **61**, R9269 (2000).
[36] S. Colson, C. J. van der Beek, M. Konczykowski, M. B. Gaifullin, Y. Matsuda, P. Gierlowski, M. Li, and P. H. Kes, Physica C **369**, 236 (2002).
[37] S. V. Dordevic, S. Komiya, Y. Ando, Y. J. Wang, and D. N. Basov, Phys. Rev. B **71**, 054503 (2005).
[38] M. Ortolani, S. Lupi, V. Morano, P. Calvani, P. Masselli, L. Maritato, M. Fujita, K. Yamada, and M. Colapietro, J. Supercon. Novel Magn. **17**, 127 (2004).
[39] V. K. ThorsmØlle, R. D. Averitt, M. P. Maley, L. N. Bulaevskii, C. Helm, and A. J. Taylor, Opt. Lett. **26**, 1292 (2001).
[40] X. G. Qiu, H. Koinuma, M. Iwasaki, T. Itoh, A. K. Sarin Kumar, M. Kawasaki, E. Saitoh, Y. Tokura, K. Takehana, G. Kido, and Y. Segawa, Appl. Phys. Lett. **78**, 506 (2001).
[41] K. M. Kojima, S. Uchida, Y. Fudamoto, and S. Tajima, Physica C **392-396**, 57 (2003).
[42] S. Uchida and K. Tamasaku, Physica C **293**, 1 (1997).
[43] S. V. Dordevic, S. Komiya, Y. Ando, and D. N. Basov, Phys. Rev. Lett. **91**, 167401 (2003).
[44] Y. Tominari, T. Kiwa, H. Murakami, M. Tonouchi, and H. Schneidewind, Appl. Phys. Lett. **80**, 3147 (2002).
[45] H. Kitano, T. Hanaguri, Y. Tsuchiyda, K. Iwaya, R. Abiru, and A. Maeda, J. Low Temp. Phys. **117**, 1241 (1999).
[46] T. Timusk and B. Statt, Rep. Prog. Phys. **62**, 61 (1999).
[47] C. Panagopoulos, J. R. Cooper, and T. Xiang, Phys. Rev. B **57**, 13422 (1998).
[48] M. B. Gaifullin, Y. Matsuda, N. Chikumoto, J. Shimoyama, and K. Kishio, Phys. Rev. Lett. **84**, 2945 (2000).
[49] C. Panagopoulos, B. D. Rainford, J. R. Cooper, W. Lo, J. L. Tallon, J. W. Loram, J. Betouras, Y. S. Wang, and C. W. Chu, Phys. Rev. B **60**, 14617 (1999).
[50] Y. T. Wang and A. M. Hermann, Physica C **335**, 134 (2000).
[51] The far (dark) sides of the small pockets have not yet been unambiguously detected, perhaps due to small quasiparticle normalization factors.
[52] T. Kondo, T. Takeuchi, A. Kaminski, S. Tsuda, and S. Shin, Phys. Rev. Lett. **98**, 267004 (2007).
[53] M. Le Tacon, A. Sacuto, A. Georges, G. Kotliar, Y. Gallais, D. Colson, and A. Forget, Nat. Phys. **2**, 537 (2006).
[54] V. L. Ginzburg, Fiz. Tverd. Tela (Leningrad) **2**, 203 (1960); [Sov. Phys. Solid State **2**, 1824 (1960)].
[55] P. M. Chaikin and T. C. Lubensky, *Principles of Condensed Matter Physics* (Cambridge University Press, Cambridge, England, 1995), Chap. 5.1.
[56] J. Tobochnik and G. V. Chester, Phys. Rev. B **20**, 3761 (1979).
[57] J. F. Fernandez, M. F. Ferreira, and J. Stankiewicz, Phys. Rev. B **34**, 292 (1986); R. Gupta, J. De Lapp, G. G. Batrouni, G. C. Fox, C. F. Baillie, and J. Apostolakis, Phys. Rev. Lett. **61**, 1996 (1988).